Colloid Polym Sci (2004) 283: 66–73
DOI 10.1007/s00396-004-1093-4

ORIGINAL CONTRIBUTION

Su Chen
Jianjun Sui
Li Chen

Positional assembly of hybrid polyurethane nanocomposites via incorporation of inorganic building blocks into organic polymer

Received: 23 January 2004
Accepted: 27 February 2004
Published online: 30 April 2004

S. Chen (✉) · J. Sui · L. Chen
School of Chemistry and Chemical Engineering, Nanjing University of Technology, 210009 Nanjing, China
E-mail: prcscn@yahoo.com.cn

Abstract Polyurethane (PU)/silica nanocomposites (PSNs) were synthesized using the "grafting from" technique by incorporation of inorganic nano-sized silica building blocks into a polyurethane matrix. Structurally well-dispersed and stable hybrids were obtained via a two-step functionalized reaction. Firstly, 3-aminopropyltriethoxysilane (APTS) was employed to encapsulate silica as the core surface. Secondly, the PU shell was tethered to the silica core surface via surface functionalization. In order to obtain complete encapsulation of silica with APTS, different ratios of APTS to silica were investigated. The mechanism of the incorporation process was also revealed. PSNs hybrids were characterized by attenuated total reflectance and Fourier transform infrared spectroscopies, differential scanning calorimetry, thermogravimetric analysis, and transmission electron microscopy.

Keywords Polyurethane/silica nanocomposites positional assembly · 3-Aminopropyltriethoxysilane · Polyurethane · Silica nanoparticles

Introduction

Assembly of inorganic-organic nanocomposite materials and associated nanoscience affords unique opportunities to create revolutionary material combinations. These novel materials can have unexpected properties arising from the synergism of the components. Increasing attention has been paid to the incorporation of an inorganic network such as a silica phase into an organic polymer matrix due to their obvious potential physical and chemical properties [1, 2, 3, 4, 5, 6]. Recent progress in new polymer synthesis techniques makes it possible to synthesize well-defined polymer-nanoparticle hybrids with novel properties and controlled architectures. There are many methods for attaching polymer chains onto nanoparticle surfaces, including chemisorption [7], covalent attachment of end-functionalized polymers to a reactive surface ("grafting to") [8], and in-situ monomer polymerization with monomer growth of polymer chains from immobilized initiators ("grafting from") [9, 10]. Current polymerization methods used to prepare inorganic/organic hybrids by tethering polymer chain to nanoparticle surfaces include anionic, cationic, ring-opening metathesis, nitroxide-mediated, atom transfer radical polymerization (ATRP) and reversible addition fragmentation chain transfer (RAFT). Some reports have described the preparation of well-defined polymer-nanoparticle hybrid using surface-initiated/living radical polymerization (SRP), such as ATRP, and living anionic surface-initiated polymerization (LASIP) [11, 12]. The most commonly employed preparation procedure for these materials is the use of the sol-gel process, which offers several advantages over other techniques. The incorporation of the inorganic network and the macrostructure of

the hybrid composite can be controlled by several synthetic parameters, such as pH value, water-to-alkoxide ratio, and temperature [13, 14].

Of these hybrid composites, polyurethanes (PUs), as the organic matrix, have received most attention for their versatile properties and a variety of starting materials. Therefore, the tailor-made properties of this class of materials can be obtained from well-designed combinations of monomeric materials. PUs can be designed to meet the diverse requirements of many materials such as elastomers, coatings, adhesives and foams [15, 16, 17]. On a molecular basis, the segmented PU may be described as the linear structure block copolymer of the $(AB)_n$ type. The part A hard segment is composed of the oligomers, which are prepared by the reaction of a low molecular weight diol or triol chain extender with diisocyanate; and the part B soft segment is normally a polyester and polyether macrogel with a molecular weight ranging from 1,000 to 3,000 [18]. Some research groups have prepared PU composites containing intercalated silicate layers [18, 19, 20, 21, 22] and silica [23, 24, 25, 26, 27, 28]. Wei et al. [18] studied the effect of organoclay concentration on the properties of PU/clay nanocomposite. They prepared PU/clay nanocomposite by using Na^+-montmorillonite treated with 12-aminolauric acid and benzidine. The twofold increase in tensile strength and threefold increase in elongation as compared to those of single PU were obtained by adding 1wt% modified organoclay in PU nanocomposites. Tortora et al. [21] extensively studied the structure and transportation properties of organically modified montmorillonite/PU nanocomposites. These nanocomposites were obtained by a three-step process using diphenylmethane diisocyanate, poly(ϵ-caprolactone), di(ethylene glycol) and poly(ϵ-caprolactone)-OMont (NPCL) nanocomposites. Martín-Martínez et al. studied PUs containing different silicas [23]. They used silicas as fillers in the thermoplastic PU composites. The physical properties of PU-silica composites and interactions between silica and PU were investigated. Pereira et al. [24] employed X-ray diffraction to characterize PU-silica composites. They investigated the influence of two kinds of silica on the crystallinity index and chain orientation. Although a lot of work has been done on incorporation of silica nanoparticles into PU, it still remains relatively unexplored with respect to the preparation of nanocomposite materials. In this work, we report that the PU/silica nanocomposites (PSNs) can be carried out by incorporating silica nanoparticles building blocks into a PU matrix. In pursuit of this, attenuated total reflectance spectroscopy (ATR), Fourier transform infrared spectroscopy (FT-IR), differential scanning calorimetry (DSC), thermogravimetric analysis (TGA), and transmission electron microscopy (TEM) were employed for the characterization.

Materials and methods

Materials All chemicals and reagents used were as follows: N220 Poly(propylene glycol) (hydroxyl number of 56 mg KOH/g, Jinlin Petrochemical), fumed spherical silica with a particle size of 21.8 nm and BET of 160 m^2/g was purchased from Mingri. 3-Aminopropyltriethoxysilane (APTS) with a wetting area of 353 m^2/g, kindly supplied by Aldrich, was used without purification. Toluene 2, 4-diisocyanate (TDI) and 1, 4-butanediol (BD) were all of analytical grade purity and used as received.

Synthesis of PU/silica grafted APTS hybrid nanocomposites The amount of APTS incorporated onto the silica surface could be calculated according to the following formula:

$$W_1 = mW_2 \times A_{SiO_2}/A_{APTS} \quad (1)$$

Table 1 Different weight ratios of 3-aminopropyltriethoxysilane (*APTS*) to silica

No.	Silica (g)	APTS (g)	Coefficient (*m*)
a	1	0	0
b	1	0.225	0.5
c	1	0.45	1.0
d	1	0.90	2.0
e	1	1.35	3.0

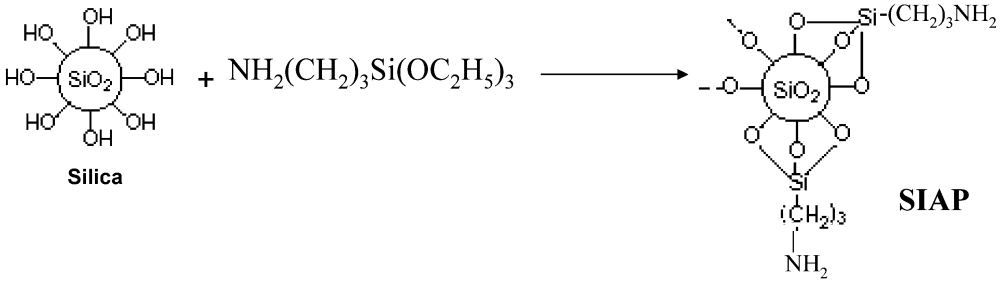

Scheme 1 Schematic formation of 3-aminopropyltriethoxysilane (APTS)-modified silica (*SIAP*) by grafting of APTS into the silica nanoparticle's surface

Table 2 The composition of PSN hybrids. *SIAP* Silica grafted APTS,*TDI* toluene 2, 4 diisocyanate, *BD* 1, 4-butanediol

Sample no.	TDI (g)	Poly(propylene glycol) (g) Mn = 2,000	BD (g)	Calculated value of APTS in SIAP (g)	Silica content (%)
1	4.35	20	0.9	0.17	1.5
2	4.35	20	0.9	0.11	1.0
3	4.35	20	0.9	0.06	0.5
4	4.35	20	0.9	0.03	0.25
5	4.35	20	0.9	0.00	1.5
6	4.35	20	0.9	0.00	1.0
7	4.35	20	0.9	0.00	0.5
8	4.35	20	0.9	0.00	0.25
9	4.35	20	0.9	0.12	0.0
10	4.52	20	0.9	0.03	0.0
11	4.35	20	1.35	0.11	1.0
12	4.52	20	0.9	0.015	0.25

Scheme 2 Schematic formation of polyurethane (PU)/SIAP hybrid nanocomposites

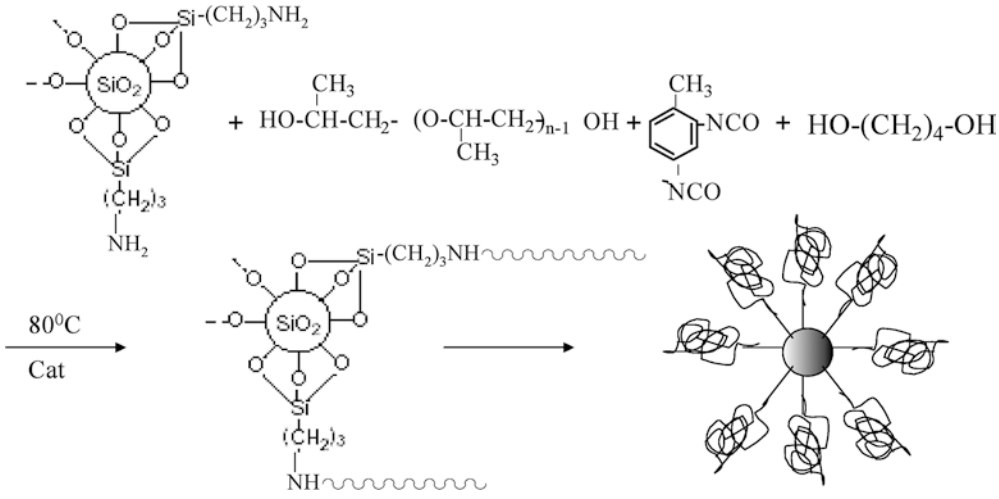

where W_1 is weight of APTS, m is the coefficient (multiple), W_2 is the weight of silica, A_{SiO2} is the specific surface area of silica (160 m^2/g), and A_{APTS} is the wetting area of APTS (353 m^2/g)

Based on the above formula, silica grafted APTS (SIAP) with different weight ratios of silica to APTS are shown in Table 1. In the present case, 10 g fumed spherical silica in 400 g toluene was refluxed with stirring at 120 °C for 2 h, then 4.5 g APTS was introduced to this solution. The mixture was refluxed for 12 h with vigorous stirring. After isolation and dehydration with methanol washing, the free APTS was removed. Finally, SIAP nanopowder was dried under vacuum. The procedure of preparing SIAPs with other weight ratios was the same as the above description. The schematic synthesis of SIAP is shown in Scheme 1. As shown in Table 2, 12 kinds of hybrid nanocomposites were synthesized. Firstly, the SIAP nanopowder was well dispersed in poly(propylene glycol). Then TDI and toluene solvent were introduced to the mixture, for the prepolymerization carried out at 85 °C for 3 h. Finally, the BD chain extender was poured into the mixture with vigorous stirring at 80 °C for 1 h. The schematic synthesis of PSN hybrids is shown in Scheme 2.

Characterization The incorporation of silica nanoparticles into PU matrix was examined by ATR-FT-IR. The FT-IR spectra were recorded in the range of

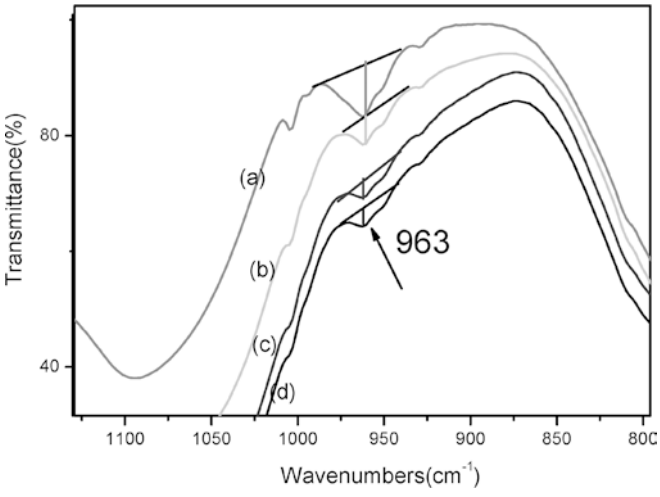

Fig. 1 Different Fourier transform infrared spectoscopy (FT-IR) characteristic peak heights of SIAP with changing weight ratios of 3-aminopropyltriethoxysilane (APTS) to silica illustrated at 963 cm; the compositions of *a*, *b*, *c*, and *d* are shown in Table 1

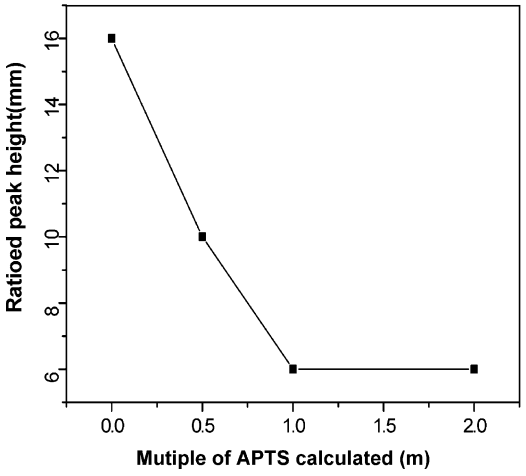

Fig. 2 Different FT-IR peak heights of SIAPs illustrated at 963 cm^{-1} vs the changing ratios of APTS to silica

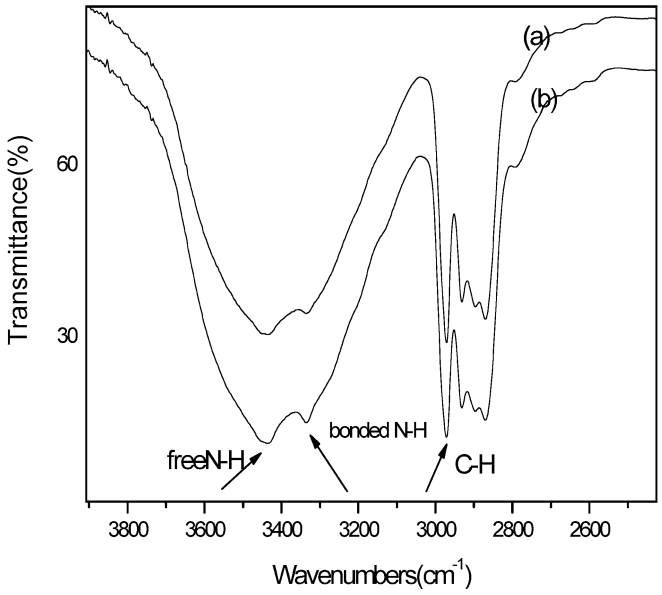

Fig. 3 FT-IR spectra of single polyurethane (PU) and PU/silica nanocomposite (PSN). *a* Single PU, *b* PSN with 2% SIAP

450–4,000 cm^{-1} with 100 scans by Perkin Elmer Model 1760x. The morphologies of the hybrid polymer nanocomposites were measured using a Hitachi 7100 transmission electron microscope. The samples for TEM observation were prepared by casting one drop of diluted solution onto a carbon-coated copper grid. The characterization by DSC was performed on a Perkin-Elmer. The samples were heated at a rate of 10 °C/min from −100 °C to 100 °C [29]. Thermal decomposition of hybrid films was determined using TGA, on a Shimadzu TGA-50 at a heating rate of 10 °C/min.

Fig. 4 Attenuated total reflectance (ATR)-FT-IR spectra changes with different contents of SIAPs. *1* 1.5% SiO_2, *2* 1% SiO_2, *3* 0.5% SiO_2, *4* 0.25% SiO_2 (the compositions of 1, 2, 3, and 4 are shown in Table 2)

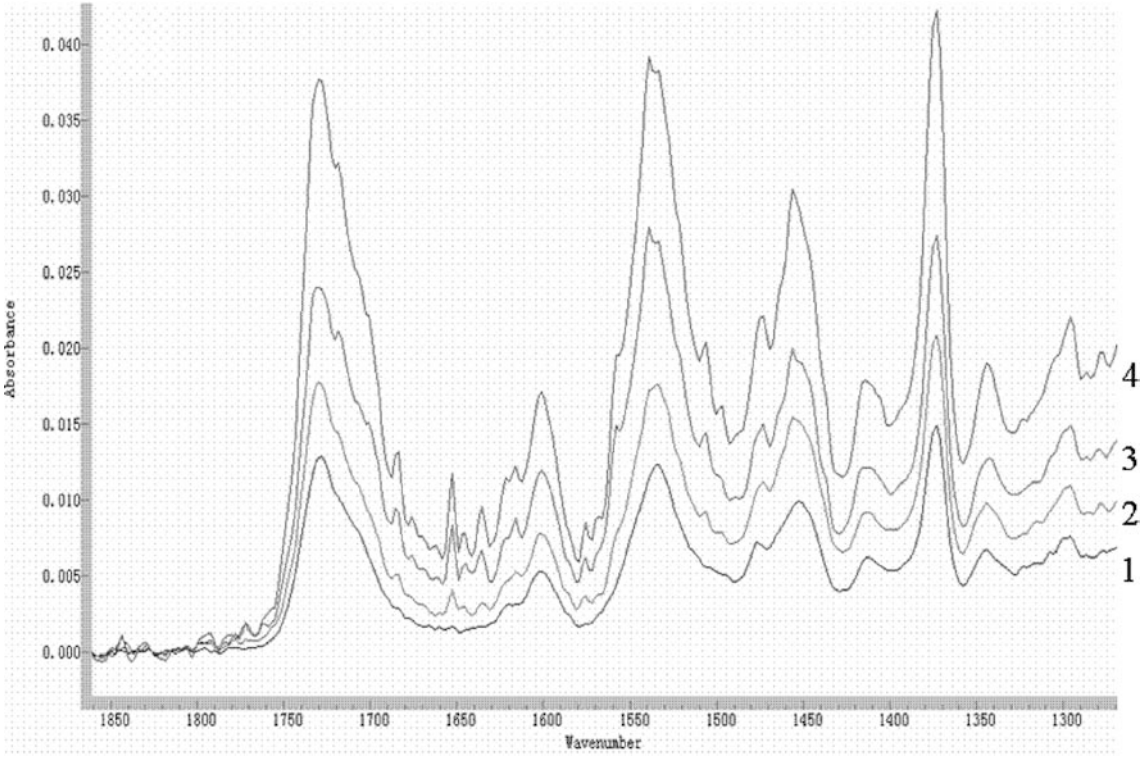

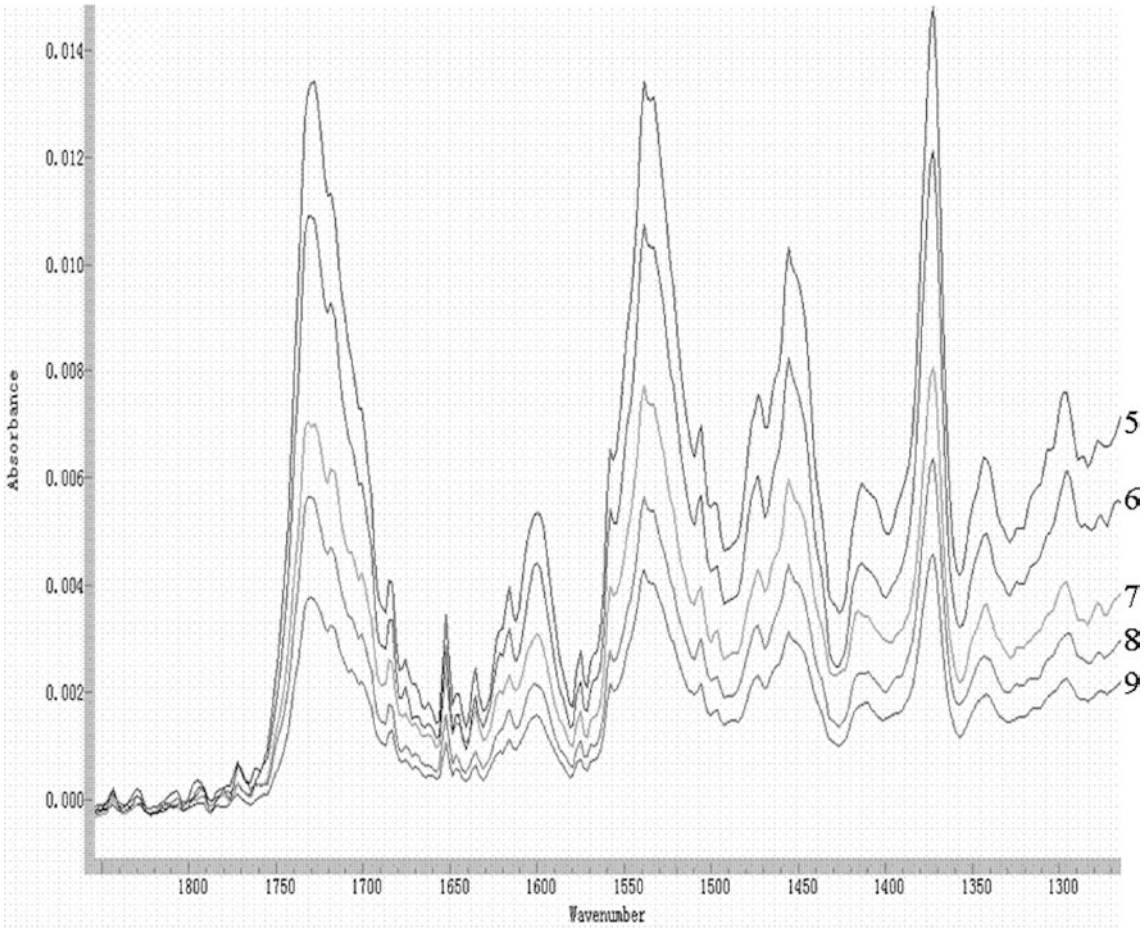

Fig. 5 ATR-FTIR PSNs spectra changes with different silica contents. *5* 1.5% SiO_2, *6* 1% SiO_2, *7* 0.5% SiO_2, *8* 0.25% SiO_2, 9. 0% SiO_2 (the compositions of 5, 7, 8, and 9 are shown in Table 2)

Results and discussion

Fabrication of PU/SIAP hybrid nanocomposites

In order to obtain complete encapsulation of silica nanoparticles with APTS, the concentration of APTS has been calculated using the formula Eq. 1 [30] with the amount of silanol groups available (12.0 μmol m^{-2}). The different stoichiometry of APTS with SiOH groups was investigated. The data are shown in Table 1. The free unreacted APTS was removed using methanol washes [30]. Scheme 1 shows that grafting of APTS onto the silica surface, which is expected to proceed in the reaction between the silanol groups of silica and the alkoxysilane functionalities, can yield amine group functionalities on the silica surface. To promote this reaction rate, adding a small amount of water into this system can be helpful for the hydrolysis of the alkoxysilane groups of APTS to silanol groups [31]. Amine groups attached to the silica core allow the subsequent grafting of PU from the silica surface moiety (shown in Scheme 2) in the respect that amine groups can easily react with NCO groups of diisocyanate to generate urea linkages. This grafting approach leads to formation of particle-like structures, which can be tailored by the size and functionality of the silica core and/or the PU shell. In this case, a key step is the encapsulation of APTS into the silica particle surface.

Materials characterization

IR characterization To gain better understanding of the encapsulation process of APTS onto the silica surface and the process of PU grafting into the modified silica surface, the IR spectra can help confirm their structure. The FT-IR spectra with different weight ratios of APTS to silica nanoparticles are presented in Fig. 1. It has been noted that the characteristic peaks of SiOH at a wave number of 963 cm^{-1} decrease with increasing APTS concentration. This can be explained by the fact that APTS was coupled with the silanol group of silica, which led to the decrease in silanol content. The different

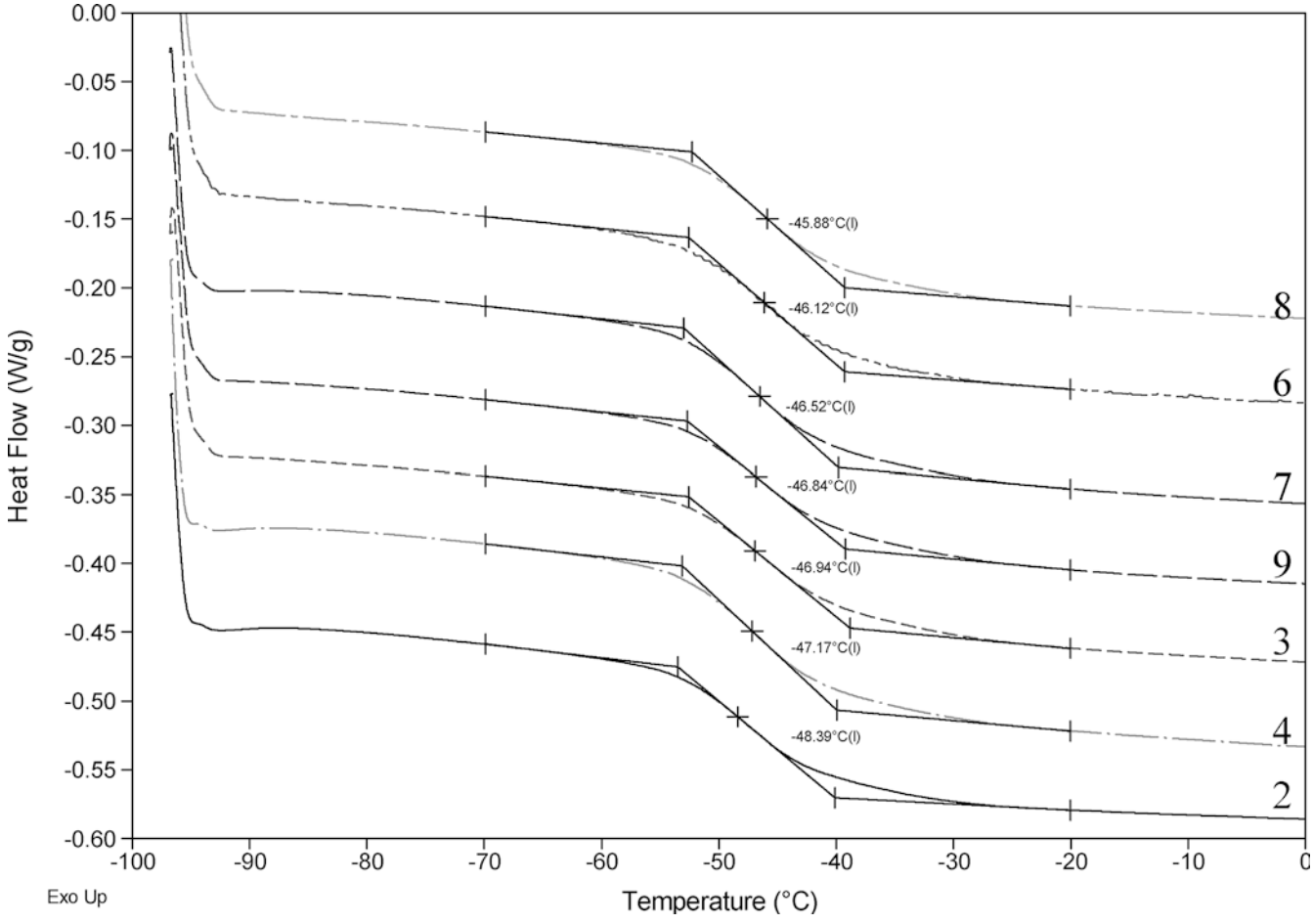

Fig. 6 Differential scanning calorimetry (DSC) glass transition temperatures (T_gs) of PSNs changes with different SIAP contents: *8* $T_g = -45.88$ °C, *6* $T_g = -46.12$ °C, *7* $T_g = -46.52$ °C, *9* $T_g = -46.84$ °C, *3* $T_g = -46.94$ °C, *4* $T_g = -47.17$ °C, *2* $T_g = -48.39$ °C (the compositions of 8, 6, 7, and 9 are shown in Table 2)

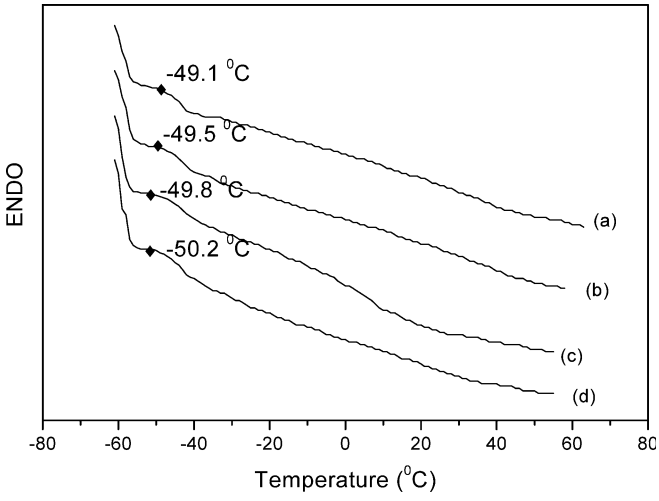

Fig. 7 DSC T_gs of PSNs changes with different compositions. *a* Single PU, *b* 1% SIAP, *c* 2% SIAP, *d* 4% SIAP

FT-IR characteristic peak heights of SIAP illustrated at 963 cm^{-1} versus the changing ratios of APTS to silica is shown in Fig. 2. Figure 2 also confirms that the peak height at the wave number of 963 cm^{-1} decreases with the increasing weight ratio of APTS to silica. Figure 3 presents FT-IR spectra of single PU and PSN. As indicated in Fig. 3, the characteristic peaks of PSNs at 3,435 cm^{-1} and 3,334 cm^{-1}, which signify free N-H groups and N-H groups of hydrogen-bonded urethane respectively, become sharp and accented compared to the IR spectrum of single PU. It is attributed to the grafting reaction between SIAP and PU. In addition, Fig. 4 shows changes in ATR-FTIR spectra with different SIAPs contents. As shown in Fig. 4, we can see the difference in PSNs' IR spectra at the wave number of 1,660 cm^{-1} with changing SIAP content. The peak of the amide groups –CO-NH- at the wave number of 1,660 cm^{-1} increased with decreasing SIAP contents. This is because diisocyanate is usually in excess in the pre-polymerization and the content of free -NCO groups decreased with increasing SIAP content. Thus, the content of –CO-NH- in hybrid films can be correlated to

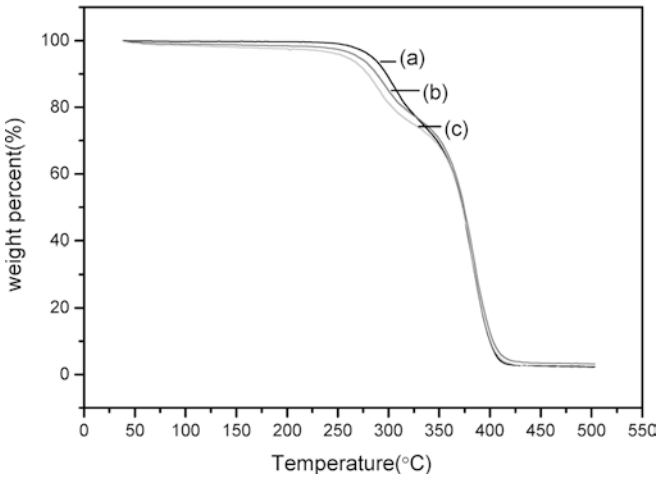

Fig. 8 Thermogravimetric analysis curves of PSNs with different SIAP contents. *a* Single PU, *b* 1% SIAP, *c* 2% SIAP

the content of free isocyanate. The same phenomena were observed for the changes in the aromatic characteristic peak shown in Fig. 4. Figure 4 shows that the aromatic characteristic peak areas at 1,616, 1,577, 1,510 and 1,456 cm^{-1} respectively are enhanced with decreasing SIAP content. In Fig. 5 are presented changes in ATR-FTIR spectra of PSN with different silica contents. As shown in Fig. 5, the IR peak heights of PSNs at 1,660 cm^{-1} do not change with increasing silica content. It means that silica without any modification has little effect on the chemical structure of PU composites. On the other hand, it is also proven that the functionalized silica is helpful for positional assembly of these hybrid PSNs.

DSC characterization of PSNs As shown in Table 1, silica contents in the recipes of no. 2 and no. 6 are the same, as are those of no. 3 and no. 7. Silica nanoparticles in the recipes of no. 2 and no. 3 are modified with APTS, while the silica nanoparticles in the recipes of no. 6 and no. 7 are without APTS modification. To compare the glass transition temperature (T_g) in Fig. 6 of curve 2 with that of curve 6, and that of curve 3 with that of curve 7 respectively, DSC pictures (shown in Fig. 6) show that T_gs of PSNs with SIAPs are lower than those of PSNs with silica nanoparticles. Also, the T_gs of PSNs increase to a very limited extent with increasing silica content. Meanwhile, T_gs of PSNs decrease slightly with increasing SIAP content. It may be associated with poor stacking among molecules when APTS was not used to modify silica nanoparticles. On the other hand, when APTS was applied to modify the silica nanoparticle surface, it could reduce the molecular interaction between inorganic particles and organic polymer. Similar results can be obtained from Fig. 7. T_gs of PSNs decrease with increasing SIAP content.

TGA characterization of PSNs The TGA curves of PSNs under nitrogen are shown in Fig. 8. It indicates that differential thermogravimetric (DTG) curves are fitted by two main degradation steps. The temperature of each stage of degradation in hybrids is attributed to scissions of the APTS organic compound and the chain of urethane. Comparing single PU with PSNs, the first platforms become wider with the addition of SIAP into PSNs. Moreover, the first platform with 2% SIAP is wider than that with 1% SIAP. Consequently, the PSNs with more SIAP content degraded less precipitously. Their rate (d Wt/d t) decreases with increasing SIAP content. These results suggest that the thermal stability of the hybrids is enhanced by the presence of SIAP.

Morphologies of PSNs The morphology of PSNs was observed directly by TEM pictures. Figure 9a shows that silica nanoparticles without APTS modification are easy to aggregate in the PSNs because of their larger surface area. The SIAP nanoparticles, however, could be well dispersed in PSNs (shown in Fig. 9b). It could be explained by the functional $-NH_2$ group of SIAP reacting with diisocyanate, allowing the silica surface to

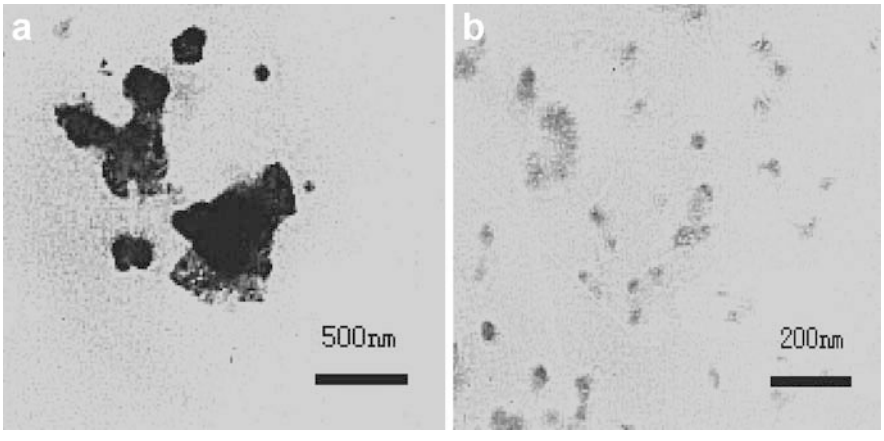

Fig. 9 Transmission electron microscopy pictures of PU hybrids with modified silica and unmodified silica. *a* PU/silica composite with the content of 2% silica, *b* PU/SIAP with the content of 2% SIAP nanoparticles

be tethered with organic PU easily, and, thus, to generate inorganic-organic core-shell particles. These inorganic-organic core-shell particles should be stable in PSNs. In addition, Fig. 8b illustrates that the particle size of silica particles in the PSN after the grafting reaction is still around 20–30 nm.

Conclusions

In the case of the assembly of hybrids of inorganic silica nanoparticles and PU matrix, optimum control over the well-defined polymer structure could be achieved by pre-assembling the silica nanoparticle with APTS and incorporation of silica inorganic building blocks into the organic PU polymer. This could be carried out via the functionalized reaction between SIAP and PU. In addition, DSC results show that the T_gs of PSNs hybrid with APTS modification are lower than those of PSNs without APTS modification. Furthermore, the functionalized silica can disperse well in the PU matrix via the grafting reaction as compared to single silica nanoparticles. Efforts should be under way to extend the utility of this methodology to other hybrid nanocomposites.

References

1. Huang HH, Orler B, Wikes GL (1987) Macromolecules 20:1322
2. Kohjiya S, Ochiai K, Yamashita S (1990) J Non-Cryst Solids 119:132
3. Morikawa A, Iyoku Y, Kakimoto M, Imai Y (1992) Polym J 24:107
4. Mascia L, Kioul A (1994) J Mater Sci Lett 13:641
5. Kim JH, Lee YM (2001) J Membr Sci 193:209
6. Park HB, Kim JK, Nam SY, Lee YM (2003)) J Membr Sci 220:59
7. Jeffrey P, Krzystof M (2001) Chem Mater 13:3436
8. Timothy VW, Timothy EP (2001) J Am Chem Soc 123:7497
9. Timothy VW, Timothy EP (1999) J Am Chem Soc 121:7409
10. Spange S (2000) Prog Polym Sci 25:781
11. Zhou Q, Wang SX, Fan XW (2002) Langmuir 18:3324
12. Chen S, Ijin Kim, Faust R (2003) J Am Chem Soc Polym Prepr 44:463
13. Chujo Y, Saegusa T (1992) Adv Polym Sci 100:11
14. Chujo Y (1996) Curr Opin Solid State Mater Sci 1:806
15. Penczek P, Frisch KC, Szczepaniak B, Rudnik E (1993) J Polym Sci Polym Chem Ed 31:1211
16. Tang W, Farries RJ, Macknight WJ, Eisenbach CD (1994) Macromolecules 27:2814
17. Kim BK, Seo JW, Jeong HM (2003) Eur Polym J 39:85
18. Chen TK, Tien YI, Wei KH (2000) Polymer 41:1345
19. Kickelbick G (2003) Prog Polym Sci 28:83
20. Yao KJ, Song M, Hourston DJ, Luo DZ (2001) Polymer 43:1017
21. Tortora M, Gorrasi G, Vittiria V, Gali G, Ritrovati S Chiellini E (2002) Polymer 43:6147
22. Tien YI, Wei KH (2001) Polymer 42:3214
23. Torró-Palau AM, Fernández-García JC, Orgilés-Barceló AC, Martín-Martínez JM (2001) Int J Adhesion Adhesives 21:1
24. Nunes RCR, Pereira RA, Fonseca JLC, Pereira MR (2001) Polym Testing 20:707
25. Kusakabe K, Yoneshige S, Morooka S (1998) J Membrane Sci 149:29
26. Nunes RCR, Fonseca JLC, Pereira MR (2000) Polym Testing 19:93
27. LeBaron PC, Wang Z, Pinnavaia TJ (1999) Appl Clay Sci 15:11
28. Gu YS, Chen L, Chen S (2003) Nanjing Gongye Daxue Xuebao 25:107
29. Chen S, Chen L (2003) Colloid Polym Sci 281:288
30. Pasquet V, Spitz R (1990) Makromol Chem 191:3087
31. Bauer F, Gläsel HJ, Decker U, Ernst H, Freyer A, Hartmann E, Sauerland V, Mehnert R (2003) Progr Org Coatings 47:147